

Design of a Commercial Hybrid VTOL UAV System

Ugur Ozdemir · Yucel Orkut Aktas · Aslihan Vuruskan · Yasin Dereli ·
Ahmed Farabi Tarhan · Karaca Demirbag · Ahmet Erdem ·
Ganime Duygu Kalaycioglu · Ibrahim Ozkol · Gokhan Inalhan

Received: 31 August 2013 / Accepted: 11 September 2013 / Published online: 8 October 2013
© Springer Science+Business Media Dordrecht 2013

Abstract For the last four decades Unmanned Air Vehicles (UAVs) have been extensively used for military operations that include tracking, surveillance, active engagement with weapons and airborne data acquisition. UAVs are also in demand commercially due to their advantages in comparison to manned vehicles. These advantages include lower manufacturing and operating costs, flexibility in configuration depending on customer request and not risking the pilot on demanding missions. Even though civilian UAVs currently constitute 3 % of the UAV market, it is estimated

that their numbers will reach up to 10 % of the UAV market within the next 5 years. Most of the civilian UAV applications require UAVs that are capable of doing a wide range of different and complementary operations within a composite mission. These operations include taking off and landing from limited runway space, while traversing the operation region in considerable cruise speed for mobile tracking applications. This is in addition to being able to traverse in low cruise speeds or being able to hover for stationary measurement and tracking. All of these complementary and but different operational capabilities point to a hybrid unmanned vehicle concept, namely the Vertical Take-Off and Landing (VTOL) UAVs. In addition, the desired UAV system needs to be cost-efficient while providing easy payload conversion for different civilian applications. In this paper, we review the preliminary design process of such a capable civilian UAV system, namely the TURAC VTOL UAV. TURAC UAV is aimed to have both vertical take-off and landing and Conventional Take-off and Landing (CTOL) capability. TURAC interchangeable payload pod and detachable wing (with potential different size variants) provides capability to perform different mission types, including long endurance and high cruise speed operations. In addition, the TURAC concept is to have two different variants. The TURAC A variant is an eco-friendly and low-noise fully electrical

Research is supported in part by the Republic of Turkey, Ministry of Science, Industry and Technology SANTEZ Program Contract 1585.STZ.2012-2 and HAVELSAN A.S.

U. Ozdemir (✉) · I. Ozkol · G. Inalhan
Faculty of Aeronautics and Astronautics,
Istanbul Technical University, 34469, Istanbul, Turkey
e-mail: ugur.ozdemir@itu.edu.tr

I. Ozkol
e-mail: ozkol@itu.edu.tr

G. Inalhan
e-mail: inalhan@itu.edu.tr

Y. O. Aktas · A. Vuruskan · Y. Dereli · A. F. Tarhan
Istanbul Technical University, 34469, Istanbul, Turkey

K. Demirbag · A. Erdem · G. D. Kalaycioglu
HAVELSAN A.S., M. Kemal Mah. 2120. Cad. No:39,
06510, Cankaya, Ankara

platform which includes 2 tilt electric motors in the front, and a fixed electric motor and ducted fan in the rear, where as the TURAC B variant is envisioned to use high energy density fuel cells for extended hovering time. In this paper, we provide the TURAC UAV's iterative design and trade-off studies which also include detailed aerodynamic and structural configuration analysis. For the aerodynamic analysis, an in-house software including graphical user interface has been developed to calculate the aerodynamic forces and moments by using the Vortex Lattice Method (VLM). Computational Fluid Dynamics (CFD) studies are performed to determine the aerodynamic effects for various configurations. For structural analysis, a Finite Element Model (FEM) of the TURAC has been prepared and its modal analysis is carried out. Maximum displacements and maximal principal stresses are calculated and used for streamlining a weight efficient fuselage design. Prototypes have been built to show success of the design at both hover and forward flight regime. In this paper, we also provide the flight management and autopilot architecture of the TURAC. The testing of the controller performance has been initiated with the prototype of TURAC. Current work focuses on the building of the full flight test prototype of the TURAC UAV and aerodynamic modeling of the transition flight.

Keywords VTOL · Tilt Rotor · Hybrid UAV · UAV Design

1 Introduction

For the last four decades, Unmanned Air Vehicles (UAVs) have been extensively used for military operations that include tracking, surveillance, active engagement with weapons and airborne data acquisition purposes. UAVs are also in demand commercially due to their low manufacturing and operating costs, flexibility in configuration depending on customer request and not risking pilot in demanding missions [1]. Nevertheless civilian UAV systems still have critical issues such as integration to the manned flight air space, certification, reliability and flight safety that need to

be fully addressed before being fully utilized in daily operations.

1.1 Commercial Application of UAVs

Even though civilian UAVs currently constitute 3 % of total UAV market, it is estimated that they will claim 10 % of the UAV market within the next 5 years [2]. UAV systems with attached payloads (hyperspectral imager, air composition sensors and similar environmental apparatus) find new areas of utilization at numerous civilian processes such as:

- Tracking and monitoring in the event of agriculture / forest / marine pollution / waste / emergency and disaster situations, [3]
- Mapping for land registry, [4]
- Wildlife and ecologic monitoring, [5]
- Traffic monitoring, [6]
- Geological and mining researches,
- Gas leakage monitoring, [7]
- Vegetation monitoring, [8–10]
- Plant and forest species identification, [11, 12]
- Climate change studies and [13]
- Environmental damage tracking [14].

UAVs bring minimal risk and cost advantage to numerous civilian applications which have once been considered as risky and costly due to the need for using manned air vehicles. Subject to the area of usage and body type, UAVs may come with various form factors such as:

- Fixed Wing UAV, [3]
- Lighter-than-air UAV, [3]
- Unconventional UAV (Quadrotor, etc.), [3]
- Vertical take-off and landing UAV, [3, 15]
- Rotating wing UAV, [3, 15]
- Tilt-rotor / Tilt-wing, [15]
- Tail-sitter and [15]
- Thrust-Reserving UAV [15].

Commercial UAV market in Europe (and in the World in general) is expected to show a continuous upward trend [16] as can be seen in Figs. 1 and 2.

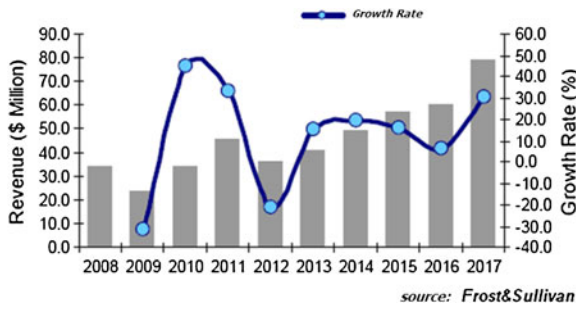


Fig. 1 Estimation of revenue of civil and commercial UAV market [16]

1.2 General Requirements for Civil UAVs

When the costs of unmanned air vehicles designed and produced for military purposes are taken into account, civil aviation market requires products oriented at its own type of processes with lower purchasing and operating costs. Most of the civilian UAV applications mentioned above require UAVs that are capable of doing a wide range of different and complementary operations as a part of a composite mission. These operations include taking off and landing from limited runway space, while traversing the operation region in considerable cruise speed for mobile tracking applications. This is in addition to being able to traverse in low cruise speeds or being able to hover for stationary measurements and tracking. All of these call for design features that provide complementary but operation wise different capabilities. In addition, such a UAV system needs to be cost-efficient while providing easy payload conversion for different civilian applications. In this paper, we provide the preliminary design process of such

Fig. 2 Estimation of revenue of European civil and commercial UAV market [16]

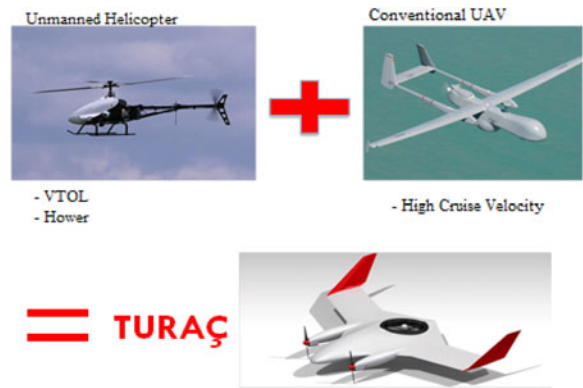
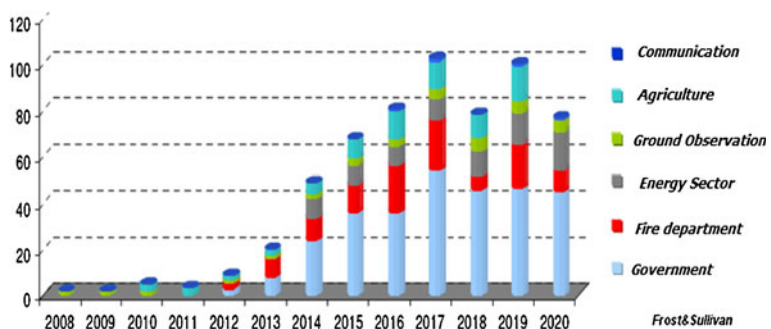


Fig. 3 The advances of TURAC VTOL UAV concept

a capable civilian UAV system, namely the TURAC VTOL UAV that has the following main features:

- Vertical take-off and landing, and hovering like a helicopter,
- Fixed-wing with high cruise speed capability and long range,
- Multi-functional and specifically designed for civilian purpose.

1.3 The Concept of VTOL UAVs

TURAC VTOL UAV is aimed at combining the advantages of unmanned helicopter and conventional UAVs (Fig. 3). VTOL UAVs have the capability of vertical take-off and landing similar to unmanned helicopters, while having high cruise speeds similar to conventional UAVs. As a result, VTOL UAVs can carry out take-off and landing operations even at hazardous environments unsuitable for standard take-off and

landing, while reaching target operation areas in a short time frame at the same time. In addition, a VTOL UAV in a cruise flight mode can change its mode to hover mode and vice versa depending on the operational requirement. All of these properties allows VTOL UAVs to realize a wider range of missions (or perform specific mission segments with higher performance) in comparison to standard unmanned helicopters and conventional UAVs [17, 18].

Helicopters hold the upper hand at the operations that require several flight modes such as switching from hover mode to cruise mode and vice-versa. VTOL UAVs can realize these operations like a helicopter. While helicopters have advantages over both VTOL and conventional aircrafts at vertical flight and backwards flight, they have performance restrictions at horizontal flight due to its low energy conversion efficiency rotors and supersonic speed limitations at rotor tips for high speed cruise. VTOL UAVs do not have these performance restrictions of helicopters in forward flight. Moreover, as long as big rotor or fan systems are not used, VTOL UAVs' mechanical designs are simpler [17, 18]. Efficiency of VTOL air vehicles at hovering is lower than helicopters due to smaller effective rotor area. However, if hovering time is considerably less than the cruise flight time, then VTOL aircrafts have higher composite efficiency due to their better cruise flight performance [17, 18].

Conventional UAVs necessitates a runway since these cannot take-off from and land to every location. However, their forward flight performances are higher than helicopter systems. While VTOL aircrafts can fly at speeds as high as conventional UAVs, additional weight due to vertical take-off/landing systems lowers their payload capacity with respect to conventional systems. Nevertheless, high thrust to weight ratio of VTOL UAVs enable better maneuvering capability than conventional UAVs. In addition, hovering and flying at low altitudes like helicopters are distinct advantages of VTOL UAVs in comparison to conventional fixed wing aircraft.

In summary, VTOL UAVs combine the advantages of helicopters and fixed-wing aircraft such as

their vertical take-off and landing capacity, high cruise speed and omnidirectional controllability. While VTOL UAVs can fly at a similar speed to fixed-wing aircraft, they can also hover like a helicopter. Even though their efficiency is lower than the vehicles that are designed for only hover flight regime or horizontal flight regime, their composite efficiency is higher because of possessing these two flight regimes [17, 18]. Evolution history of VTOL systems [18], developed VTOL UAV Design Technology [17], existing criterions [18], comparison with conventional and helicopter systems [17, 18], and future prediction [17] can be reached through the associated references.

In the next chapter, we review the design of the TURAC VTOL UAV. The design process includes further insight on TURAC Concept, target performances, comparison with existing systems, Section 2 also includes the critical sizing and design selections associated with structures, aerodynamics and power systems. Sections 3 and 4 provides details on the aerodynamic and structural analysis associated with configuration management. TURAC avionics system design including the control system structure is presented in Section 5.

2 Design of the TURAC VTOL UAV

2.1 The Concept of the TURAC UAV

The TURAC UAV is designed to be able to take off and land both conventionally and vertically. In addition, the following requirements are taken into account for the UAV to be designed and manufactured:

- Lower cost than similar military UAVs,
- Vertical take-off and landing capability,
- Conventional take-off and landing capability,
- Hovering capability,
- Eco-friendly and low noise electrical power system,
- Ease of portability and packaging,
- Ability to work with different kinds of payloads and

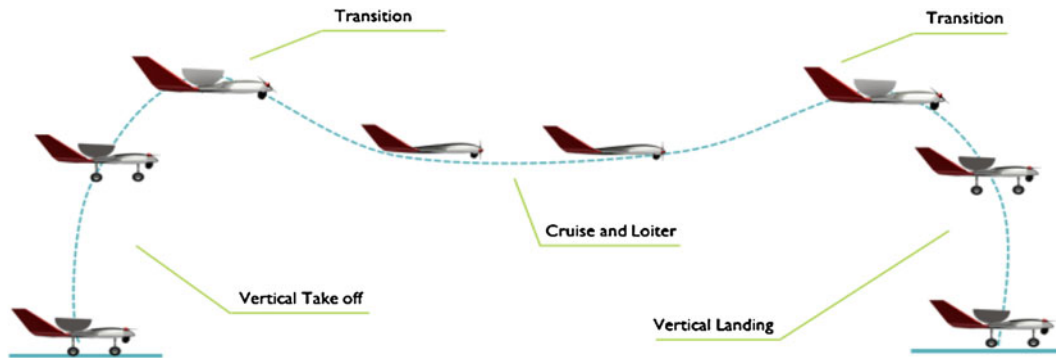


Fig. 4 Flight mission profile

- Highly mobile and compact ground station.

In addition to these requirements, minimum target performance criterions for TURAC VTOL UAV are given as follows:

- 1 hr cruise + 10 min hovering + 15 min take-off and landing,
- 35 km operation radius (70 km range),
- 8 kg payload (hyperspectral imager or potentially additional devices such as RGB camera, thermal camera, emission measurement device),
- 20 m/s cruise speed and
- Automatic take-off, landing and flight system.

The above requirements and minimum target performance criterions are based on typical mission scenarios as noted in Section 1. The typical mission profile of the TURAC which includes vertical take-off, transition to cruise, cruise, transition to hover and vertical landing can be seen in Fig. 4.

The TURAC UAV conceptual design in Fig. 5 was conceived by taking the noted requirements into consideration. In this concept, the TURAC UAV includes 2 tilt rotors which are active during all of the flight phases and also one main rotor which is just active during the VTOL and hovering phase. On aircraft mode, tilt motors are turned to flight direction step by step, and the power of co-axial motors is boosted simultaneously in order to create necessary lifting force. Wings create lifting force as UAV accelerates, and the power of co-axial motors is lowered inversely proportionally to

the lifting force. Co-axial fans with dual and distinct electrical engines stop when the lifting force is at least equal to the weight of UAV acquired from wings aerodynamically, and then front tilt motors will complete their rotation to the flight direction. Operation from cruise flight to hover is realized at the exact opposite way until stall speed is reached.

Portability is at the forefront in TURAC concept. In the design process, a concept that allows detachable aircraft wings (as well as ability to use wings with various dimensions as seen in Fig. 6) and replaceable body parts is used as the main design basis. TURAC system, which consists of two parts, namely main body and edge wings, can be mounted easily and it can be fitted in a considerably small volume with respect to its size. This way, it can be easily transported with vehicles such as SUV and truck. TURAC behaves like a

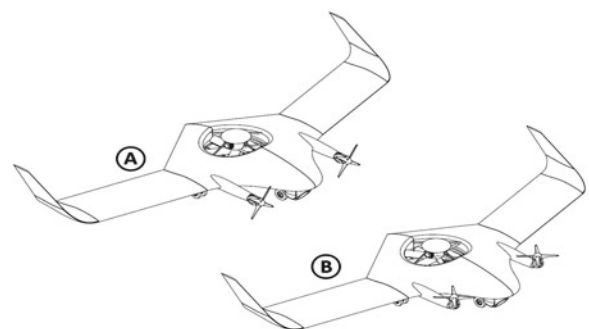


Fig. 5 The Design concept of the TURAC in cruise (a) and hover (b) mode



Fig. 6 The usage of the TURAC with varying wing size



multi-rotor system when detachable wing system is not plugged, whereas it behaves like an aircraft that can make vertical take-off and landing and hover when is the wing system is plugged. Therefore, multiple solutions and UAV types are achieved in a single device.

The TURAC VTOL UAV, which can adapt to different mission conditions with its properties given above, can take-off from and land to partly flattened dirt runways, or can start its mission by taking off from ships or land patches if desired.

The complete TURAC UAV System consists of two parts, which are the ground station and the air vehicle as seen in Fig. 5. Ground station consists of a ruggedized laptop used for loading missions, monitoring vehicle status and actively controlling the payload. The ground station also includes a radio command for direct remote piloting and dual transceivers for mission and payload communications

On the air vehicle, there is a flight control computer that controls all of the phases of the flight. In addition, tied to the flight computer, there are sensors with temperature compensators and filters, actuators and radio transceivers. The

Table 2 Comparison of TURAC with a CTOL UAV

	 Northrop Grumman Bat	 TURAC CTOL
MTOW (kg)	34	47
Payload (kg)	12	8
$W_{\text{Payload}}/W_{\text{MTOW}}$	0,35	0,17
Endurance (h)	8	3,25
Hover (min)	0	0
Productivity (kg*h)	96	40
Power source	ICE	Electric

flight control computer is linked to a mission management computer and payload system with its distinct computer and sensors. The mission management computer and payload system carries distinct transceivers for communications with the ground station.




2.2 Target Performance and Competitor Analysis

The comparison of the target performance of the TURAC with other best-in-class VTOL UAVs can be seen in Table 1.

The comparison of the target performance of the TURAC at CTOL phase with a best-in-class CTOL blended wing UAV can be seen in Table 2.

When compared to other VTOL UAVs, including Organic Air Vehicles I, II [19], the target performance of TURAC is superior. Specifically TURAC is depicted as being a high speed mini UAV system platform while providing considerable portability and payload capacity. As it is upgradable in terms of design, it is a basic product

Table 1 Comparison of TURAC with other VTOL UAVs

Specification	 IAI panther	 IAI mini panther	 TURAC (VTOL)
MTOW (kg)	65	12	47
Payload (kg)	8,5	2	8
$W_{\text{Payload}}/W_{\text{MTOW}}$	0,13	0,16	0,17
Endurance (h)	4	1,5	1,42
Hover time (min)	3	3	10
Productivity (kg*h)	34	3	16
Power source	Electric	Electric	Electric

which can have higher endurance with additional battery systems. “Productivity”, which is directly linked to endurance and payload capacity, is an important performance parameter for UAVs [20]. TURAC carries the best “Productivity” value within its class. In addition, basic performance parameters of competitor VTOL UAVs in comparison to TURAC are shown in Figs. 7, 8 and 9.

As seen in Figs. 7, 8 and 9, in comparison to Organic Air Vehicles, TURAC UAV aims at substantially higher range and payload carrying capacity as a result of its considerably larger size. Moreover, TURAC is designed to carry the same payload with less MTOW in comparison to IAI Panther, which is currently one of the best examples of its class within the market. Focusing on Table 2, it is apparent that all electrical TURAC is inferior to CTOL blended wing UAVs with internal combustion engines as far as endurance and payload capacity is concerned. However, TURAC brings the valuable hover, VTOL and transition capability which cannot be achieved by its conventional counterparts.

2.3 Design Process of TURAC

The design process of TURAC VTOL UAV is depicted at Fig. 10. Specifically; similar systems are investigated by taking operational, technical, and design requirements into consideration. The most efficient configuration selection process in conformance to these requirements is realized. Sizing process is repeated iteratively according to weight in accordance with selected propul-

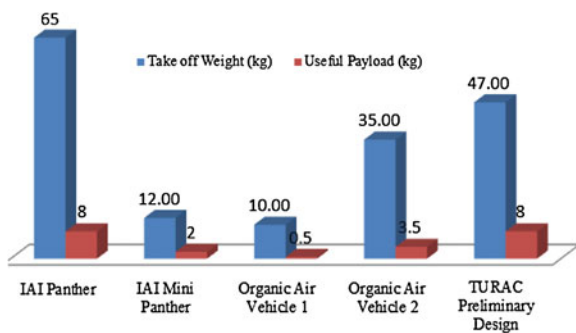


Fig. 7 Take-off weight and payload comparison

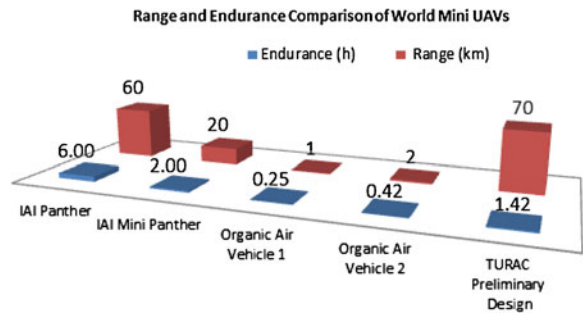


Fig. 8 Range and endurance comparison

sion system, aerodynamic and structural analyses. The results of first weight estimation and some trade-off studies can be seen in the following subsections.

In the next subsections, we review the most critical systems and selections that shape the design process. The first system analyzed is the propulsion configuration selection and controllability. Later this is followed by airfoil and wing geometry, weight and power sizing. The last subsection includes the detailed sizing including the final overall size of TURAC at the end of the iterative process.

2.4 Propulsion Configuration of the TURAC and Controllability

TURAC UAV concept includes two tilt rotors which are active during all of the flight phases and also one main rotor which is just active during

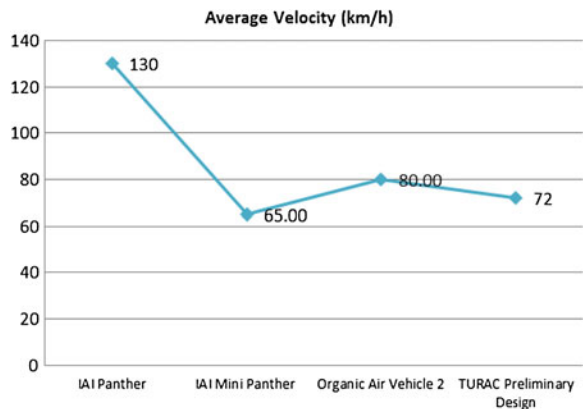
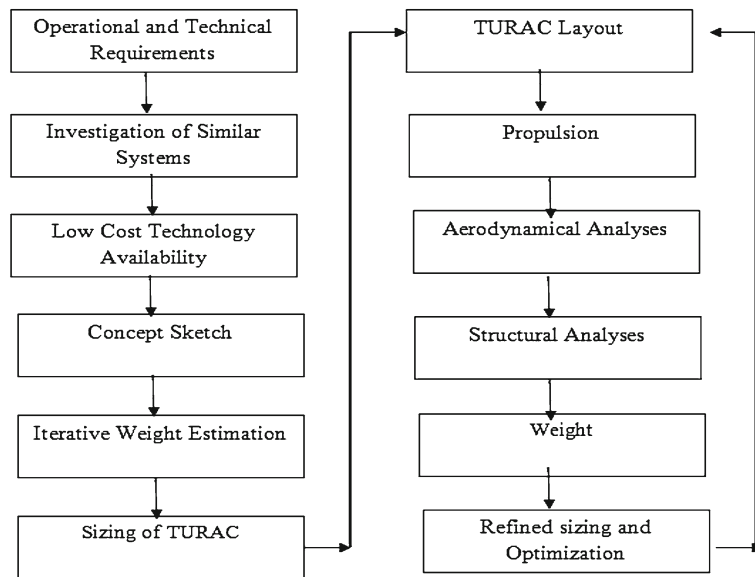
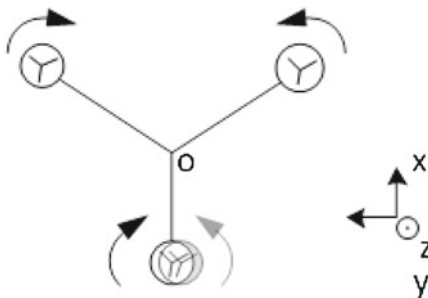


Fig. 9 Average velocity comparison

Fig. 10 Design process of TURAC

the VTOL phase. On aircraft mode, tilt motors are turned to flight direction step by step, and the power of co-axial motors is boosted simultaneously in order to create necessary lifting force. Wings create lifting force as UAV accelerates, and the power of co-axial motors is lowered inversely proportionally to the lifting force. Co-axial fans with dual engines stop when the lifting force is at least equal to the weight of UAV acquired from wings aerodynamically, and then front tilt motors will complete their rotation to the flight direction. Operation from cruise flight to hover is realized at the exact opposite way.

As it can be seen in Fig. 11, coaxial blowers function simultaneously with two tilt motors and

**Fig. 11** Compensation of moments

propellers at the front for vertical take-off and landing mode as well as hover mode. The dual tilt rotor configuration resolves the imbalance problem that is seen in a single coaxial fan system with non-aligned rotation/force axis and gravity center.

By tilting the tilt motor systems in the front, transition from hover mode to level flight to the front direction or low speed level flight to the back direction can be achieved. On the hover mode, coaxial fans can instantaneously create 70–80 % of the lifting force necessary and tilt motor system creates 10–30 % of the lifting force (Fig. 12). This flexibility allows constant stabilization in situations such as equipment placement to the center of gravity, different fuel, mission and flight conditions. Therefore, main stabilization problem for coaxial systems is solved.

Developed coaxial fan and front tilt motor and propeller system (Fig. 13) can be placed at any orientation on the aircraft without taking any issue other than stability into consideration. As a result, there is no need for specific placement angle for fan and propeller placement that is required for systems with a single fan.

Turning left or right at hover flight is accomplished by creating a torque, which is achieved by slowing down one of the coaxial fans while speeding up the other one. The total thrust level is not decreased during a turning operation due

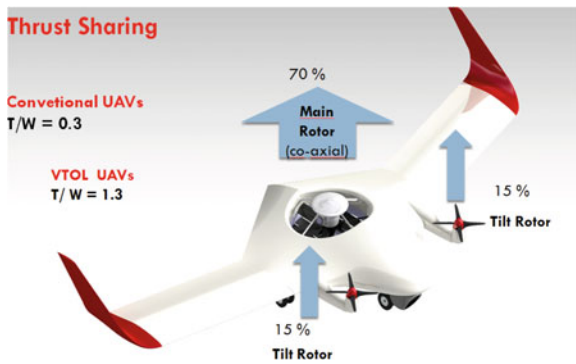


Fig. 12 Thrust sharing through rotors

to synchronized speeding up and slowing down. For rolling movement to right or left, the speed of one of the front tilt motor propellers is decreased while the speed of the other one is increased to create a rolling moment to left or right is created. The total thrust level is not decreased while doing a rolling operation because of synchronized speeding up and slowing down.

Pitching to front or to back at hover position is accomplished by creating a pitching moment, which is achieved by slowing down the set of the coaxial fans or the front tilt rotors, and speeding up the other one in combination. As the total thrust level is not reduced during a pitching operation due to synchronized speeding up and slowing down, aircraft does not destabilize.

Main lift fan power consumption is the most important issue for the optimization of hover endurance. TURAC system uses a dual engine ducted fan system with coaxial rotors which enhance the aerodynamic performance of system as

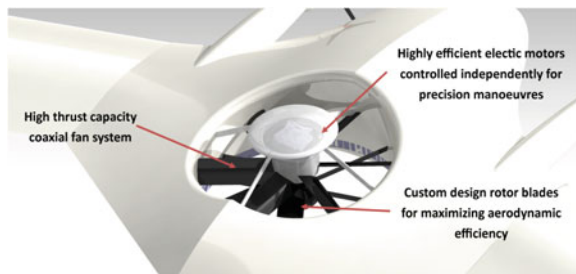


Fig. 13 Ducted co-axial fan system with dual electrical engines for extensive controllability

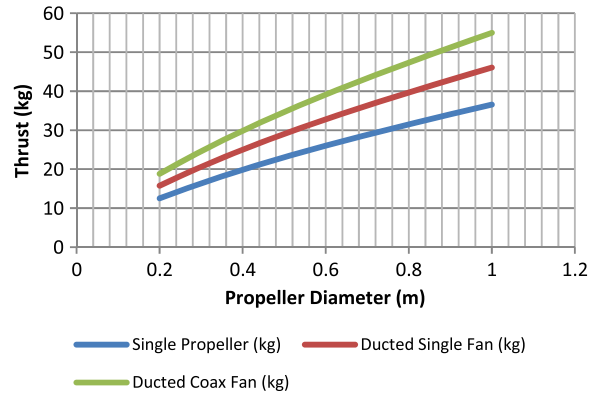


Fig. 14 Main lift fan diameter vs generated thrust comparison for various propeller and duct configurations

shown in Fig. 14. Performance calculations are based on momentum theory and flight tunnel tests with single propeller, ducted propeller and ducted coaxial propellers [20]. Figure 14 shows the thrust level of single propeller, ducted single

Table 3 Airfoil selections

	Center airfoil	NACA 34115
	Design CL	0,5
	Camber position & Reflex	20 % reflex
	Thickness (%)	15 %
	Wing airfoil	NACA 34112
	Design CL	0,5
	Camber position & Reflex	20 % reflex
	Thickness (%)	12 %
	Winglet airfoil	NACA 04012
	Design CL	0,5
	Camber position & Reflex	20 % standard
	Thickness (%)	12 %

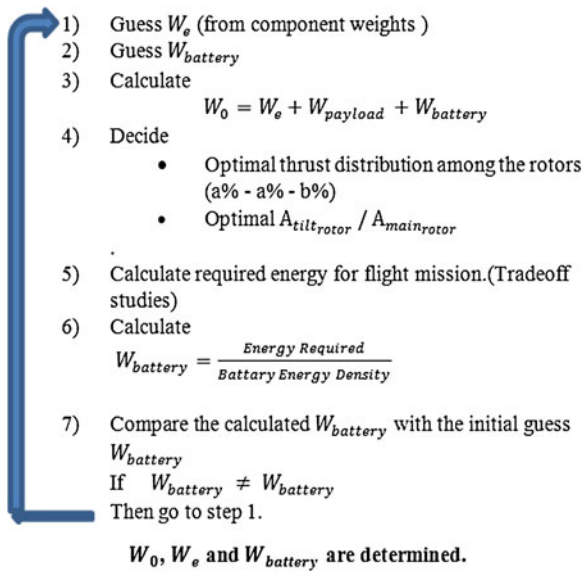


Fig. 15 Iterative weight estimation process

fan and ducted coaxial fan by using same amount of energy, respectively. Since the radius of the propellers are restricted in our concept design, obtaining high level thrust is important and thus a coaxial fan system is selected.

2.5 Airfoil and Wing Geometry

1) Wing Geometry

TURAC is a blended wing design and lift is generated from both fuselage and attachable wings. There is no tail structure to balance moment over the airfoil. For this reason, reflex airfoils are used on aircraft to balance moments which occur from generating lift. Different reflex airfoils are analyzed for TURAC as to enhance

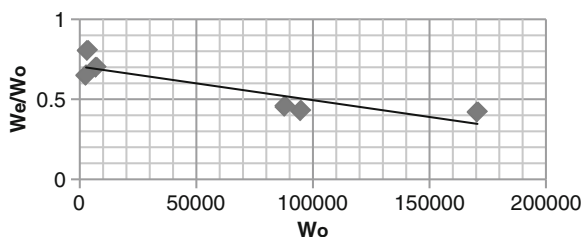


Fig. 16 Historical W_e / W_o data

Table 4 Initial weight estimation for iteration

Structures	7 kg
Avionics	5 kg
Payload	8 kg
Battery	20 kg
Motor + ESC	5 kg
MTOW	45 kg

lift capacity while holding the drag at an acceptable level. Wing shaped fuselage and attachable wings are designed with swept wing for making TURAC more stable. In addition, winglets are used to make aircraft aerodynamically more efficient. Winglets also house the rudder control surfaces for controlling yaw and coordinated roll-yaw maneuvers.

Blended wing design of TURAC provides a considerably larger usable interior space in comparison to conventional wing-body systems, and thus allows the user to mount different payloads with a wide range of sizes. As the aircraft acquires lifting force from the entire structure, it can also carry more payloads compared to similar sized aircrafts. Different sized wings can be plugged to TURAC UAV according to different performance criteria and missions. Moreover, with its wingless form (i.e. the form with no wings attached), it can work like a tri-copter (Fig. 11).

Wing sizing process is completed after estimating maximum take-off weight. The primary point of attention while making wing sizing calculations is the stall speed since TURAC performs vertical take-off/landing and forward flight and stall speeds play a crucial role in transitions. Aircraft needs to slow down until tilted propeller and main lift fan function effectively for vertical flight. At this point, stall speed is determined and sizing calculations are done.

Table 5 Required energy for all flight mission

	Duration(min)	Energy (Wh)
VTOL	10	2040.80
Climb	7.5	362.73
Cruise	60	1025.96
Descend	7.5	69.81
Total	85	3499.30

Table 6 Current battery technology

Battery brand	Max amps	ZIPPY flightmax 8400 mAh 3S2P 30C	Turnigy nano-tech 8000 mAh 6S 25 ~ 50C
Number of cells	6	3 × 2	6
Unit weight (kg)	1,22	0,772	1,111
Capacity (mAh)	11000	8400	8000
Voltage	22,2	9,9	22,2
Power (Wh)	244,2	83,16	177,6
Power density (Wh/kg)	200,16	107,72	159,85

2) Airfoil Geometry

TURAC system is an aerial platform with a tailless blended wing design. In conventional designs with standard wing profiles, the nose-down moment created by the airfoil is balanced by a tail structure. As TURAC concept is a tailless air vehicle, it requires special wing profiles that do not create nose down moments. For this reason, wing profile chosen for TURAC is a type of wing profile called reflex profile. Table 3 shows the selected reflex airfoils with the first one corresponding to the body airfoil (with higher thickness), the second one corresponding to the wing airfoil. The body airfoil transitions from NACA34115 to NACA34112 from mid to tip section to blend into the wing airfoil. The last airfoil presented within Table 3 corresponds to the airfoil for winglets.

2.6 Weight Estimation and Power Sizing

Weight estimation of TURAC VTOL UAV is an iterative process and it is given below in Fig. 15.

Stepping through the iteration step-by-step; the graphic for W_e/W_o is obtained from historical data of flying wing and blended wing systems given in Fig. 16. Looking at historical data, W_e/W_o ratio is between 0.6 to 0.8 for aircrafts with less than 100 kg weight. We expect the ratio of empty weight to MTOW to be 0.8 since power will be provided by an all electrical and battery fed system which is indeed a lower energy density system (for MTOW more than 15–20 kgs under current technology) in comparison to internal combustion engine systems.

One of the design requirements of the UAV is to carry a payload of 8 kg weight. As W_e/W_o ratio is about 0.8 at Eq. 1, then W_o can be found 40 kg by using the formula below:

$$\frac{W_o - 8}{W_o} = 0.8 \tag{1}$$

However, for the initial weight estimate needed to start the iterative process, we have to add extra system weight (5 kg), because our system is a VTOL concept and it has more weight than CTOL vehicles because of the extra lifting fan systems and structures. Thereby, our starting weight guess will be $W_o = 45$ kg.

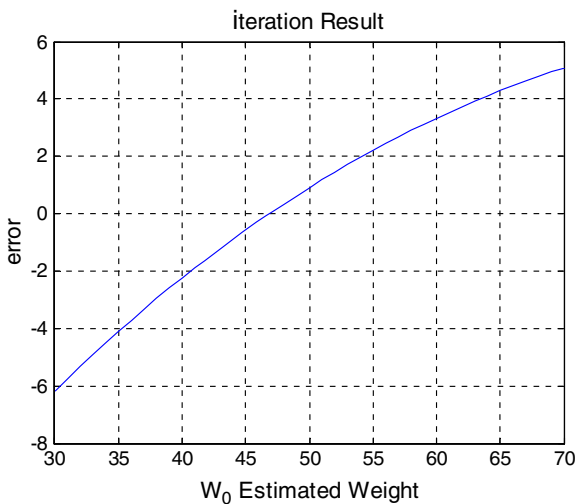


Fig. 17 Iteration error for weights

Table 7 Weight distribution

Structure	7 kg
Avionics	5 kg
Battery	22 kg
Propulsion	5 kg
Payload	8 kg
MTOW	47 kg

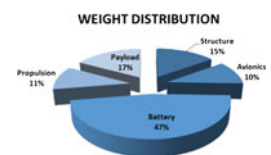


Table 8 Payload versus MTOW

W_{payload} (kg)	W_0 (kg)
3	32.5
4	35.2
5	37.8
6	40.5
7	43.6
8	47.0
9	50.4
10	54.1

Estimation of weight distribution of TURAC UAV components is given in the Table 4.

The most important factor in the determination of weight is battery weight. This is directly related to the expected missions and mission durations of TURAC UAV.

Aerial platform’s required power for the duration of mission is calculated by momentum theory, a method when fast and acceptable solutions are sought.

Power calculation for single propeller is calculated from Eq. 2.

$$P = \frac{1}{FM} \frac{T^{\frac{3}{2}}}{\sqrt{2\rho A}} \tag{2}$$

Power calculation for ducted fan can be seen at Eq. 3.

$$P = \frac{1}{FM} \frac{T^{\frac{3}{2}}}{\sqrt{4\rho A}} \tag{3}$$

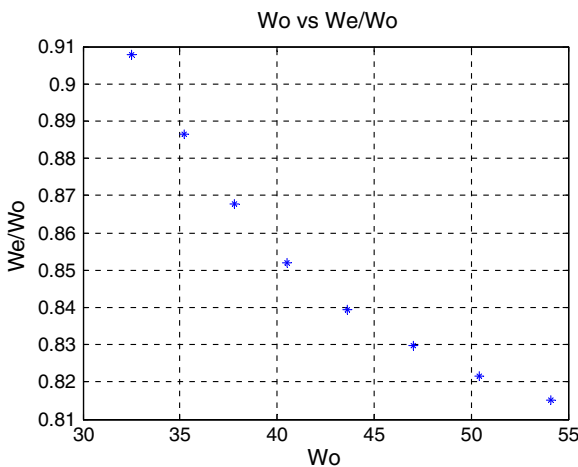


Fig. 18 W_e/W_0 versus W_0

Table 9 Optimum ratio of propeller areas

$\frac{Area_{\text{main_rotor}}}{Area_{\text{tilt_rotor}}}$	Thrust distributions		
1.0	25 %	25 %	50 %
1.5	20 %	20 %	60 %
2.0	16.5 %	16.5 %	67 %
2.3	15 %	15 %	70 %
3.0	12.5 %	12.5 %	75 %

Total energy for full mission for the first estimated weight is calculated from Eq. 4, required energy for the entire flight mission can be seen at Table 5.

$$E_{\text{total}} = E_{\text{total_VTOL}} + E_{\text{total_climb}} + E_{\text{total_cruise}} + E_{\text{total_descend}} \tag{4}$$

Battery weight can be calculated from Eq. 5 by using the data given at Table 6.

$$W_{\text{battery}} = \frac{\text{Total required energy (Wh)}}{\text{Battery Power Density} \times 0,85} \tag{5}$$

For preserving battery life of LiPo batteries, battery consumption prior to recharging should be no less than 85 % of full capacity. This, in turn, directly influences battery weight.

Selected battery system 11000 mAh, 22.2 V capacity, 6 cells LiPo battery system from Max-Amps Company, which produces battery systems for professional model aircrafts and unmanned aerial vehicles.

This process is repeated until calculated W_{battery} value is equal to the estimated W_{battery} value. At the end of iterations, iteration error at the point where W_{MTOW} equals to 47 kg is close to zero (Fig. 17).

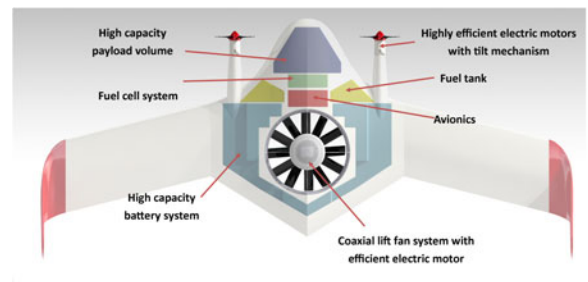


Fig. 19 TURAC design layout properties

Table 10 Sizing results of TURAC

General sizing	Length	1,8 m	
	Wingspan	4,2 m	
	Height	1,05 m	
	Wing area	3,36 m ²	
	Empty weight	39 kg	
	MTOW	47 kg	
	Aspect ratio	5,25	
	Mean chord	0,8 m	
	Propeller diameter	0,43 m	
	Aerodynamic center*	0,822 m	
	Center of gravity *	0,806 m	
	Fuselage	Center airfoil	NACA 34115
		Tip airfoil	NACA 34112
		Fuselage length	1,8 m
Fuselage span		1,6 m	
Center chord		1,8 m	
Tip chord		0,58 m	
Taper ratio		0,322	
Wing**	Root airfoil	NACA 34112	
	Tip airfoil	NACA 34112	
	Chord	0,58 m	
	Span	1,2 m	
	Swept	20°	
	Elevon length	1 m	
	Elevon width	0,145 m	
Winglet	Airfoil	NACA 04012	
	Length	0,634 m	
	Area	0,313 m ²	
	Swept (LE)	38°	
	Root chord	0,7 m	
	Tip chord	0,278 m	
	Aspect ratio	1,5	
	Taper ratio	0,397	
	Rudder length	0,5 m	
	Rudder tip width	0,111 m	
	Rudder root width	0,28 m	
Landing gear***	Height	0,421 m	
	Front LG distance	0,4 m	
	Main LG distance	0,897 m	

*Distance from center chord's leading edge

**Wing consists of 2 attachable parts, results for each part

***Distance from center chord's leading edge

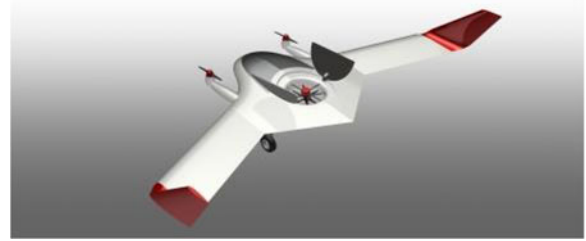


Fig. 20 TURAC in VTOL mode (open fan)

Results after the iteration process are given in Table 7.

This process can be done for different payload sizes to obtain the payload weight-MTOW trade-off. The iteration will give different MTOW results for different payloads (Table 8).

Ratio of total weight to empty weight is shown at Fig. 18. The TURAC concept is envisioned to have a B variant which uses high energy density fuel cells for extended hovering time or in turn less battery weight in favor of larger payloads.

2.7 Detailed Sizing

1) Wing Loading (W / S) – Wing Area

At take-off and landing, flight speed of aerial vehicle is close to stall speed. Thereby, calculations must be carried out considering the fact that flight speed at maximum load is equal to stall speed.

V_{stall} is regarded as 20 m/s, and calculations are done for 18 m/s as a safe approach. For W_{MTOW} equals 47 kg, $C_{L_{max}}$ equals 0.7 and ρ equals 1.121.

$$L = \frac{1}{2} \rho V^2 S C_L \tag{6}$$



Fig. 21 TURAC in cruise mode (closed fan)

Table 11 Performance results

Mission profile		Thrust distribution	
Starting altitude	0 m	1. Tilt thruster	15 %
Mission altitude	1000 m	2. Tilt thruster	15 %
		Main thruster	70 %
VTOL		CTOL	
Flight mode	Time (min)	Flight mode	Time (min)
VTOL	10	VTOL	–
Climb	7,5	Climb	7,5
Cruise	60	Cruise	180
Descent	7,5	Descent	7,5
Total	85 min	Total	195 min

By using Eq. 6, the value of S is calculated 3.36 m^2 and W/S ratio is also calculated 13.39 kg/m^2 , which is indeed considerably low wing loading for such UAVs.

2) Taper Ratio

Taper ratio at body is given at Eq. 7.

$$\lambda_{\text{body}} = \frac{C_{\text{body root}}}{C_{\text{body tip}}} = \frac{1.8}{0.58} = 0.32 \quad (7)$$

Tapering method is not implemented for interchangeable wings. Thus, tapering ratio is taken as 1 according to Eq. 8.

$$\lambda_{\text{wing}} = \frac{C_{\text{root}}}{C_{\text{tip}}} = \frac{0.58}{0.58} = 1 \quad (8)$$

3) Sweep Angle:

TURAC system will be affected from disturbances occurring at air substantially because of the increasing wing loads. For this reason, work for increasing stability at rotation axis is carried out by giving 20° sweep angle to the wings. The loss of lift due to sweeping is partially tolerated by using winglet.

4) The Ratio of Propeller Areas

The required energies for the given mission are calculated for different ratios of the propeller to reach optimum ratio of propeller areas (Table 9).

As seen from Table 9, the best area ratio is 2.3 for (15 % –15 % –%70) distribution of thrust which should be provided by tilt rotors and main rotor, respectively.

5) Inner Volume Allocation of TURAC

Inner volume allocation properties of TURAC VTOL UAV B variant are given at Fig. 19. The TURAC B variant includes the fuel cell and the fuel tank system. In the A Variant this is replaced with further battery cells. In the inner volume allocation, main transportation fan is close to the middle section of the vehicle. Front electric motors directed upwards during VTOL phase stabilize vehicle during hover and are used at cruise flight.

Battery system near main duct can be completely removed and replaced from the aircraft to ensure preparation of the vehicle for immediate follow-up missions. Lithium Polymer battery system, which has the highest energy density and is commercially available, is chosen as battery system. Fuel tanks made of Kevlar and located near to the center of gravity and work with fuel cell system for alternative electric power generation.

6) TURAC Sizing Results

Results found from calculations are given at Table 10.

The drawing of TURAC in hover and cruise modes according to sizing calculation can be seen in Figs. 20 and 21 respectively.

7) Performance Results

Performance results of the design can be seen in Table 11.

3 Aerodynamic Analysis of TURAC

For the aerodynamic performance and configuration analysis an in-house code is developed

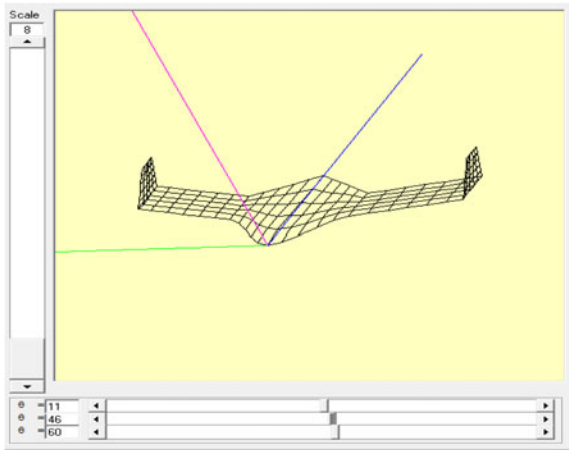


Fig. 22 The GUI of the developed code for parametric aerodynamic analysis of TURAC

using the vortex lattice method. This analysis provided us with a general understanding of lift, moment and induced drag values of various aerodynamic configurations. Later these analyses are verified by using CFD methods.

3.1 The Developed Code for Aerodynamic Analyses

As the initial step of the analysis, a parameterized size model of the TURAC is created. The model

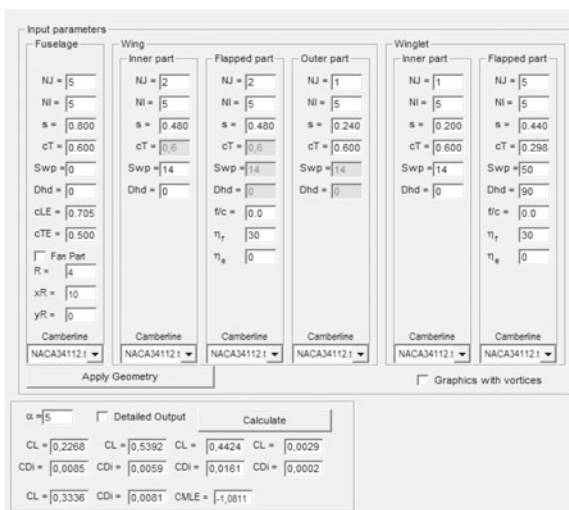


Fig. 23 The GUI of the developed code for VLM

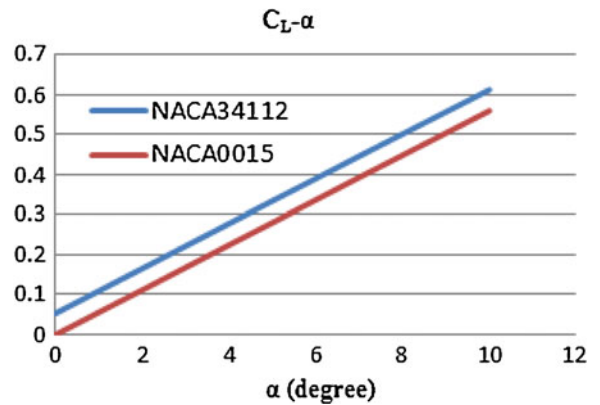


Fig. 24 Lift coefficient versus angle of attach

includes a numeric description of the wings, control surfaces and winglets.

In developed code, Vortex Lattice Method (VLM) is used by separating UAV geometry to small panels. The geometry of TURAC is created by using defined parameters; each component is separated to a number of panels according to user’s desire and C_L , C_{Dind} and C_M are calculated for each component of TURAC and full geometry by using VLM. Geometry and panel parameters can be changed easily through the user interface of the developed code. The user interface of the developed code can be seen in Figs. 22 and 23. It also imposes the effect of fan chamber, rudders and flaps in the calculation.

At VLM, each panel is symbolized with horseshoe vortex. Horseshoe vortex starts at one quar-

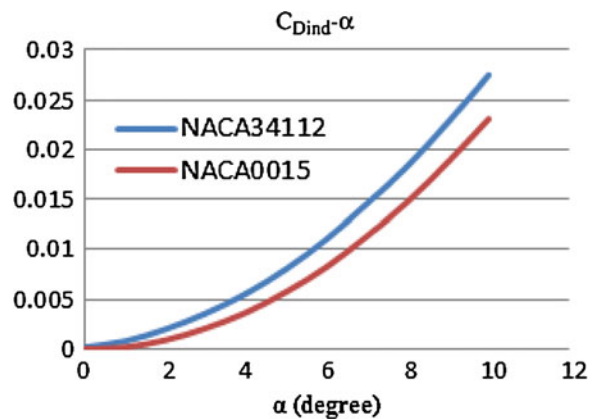


Fig. 25 Induced drag versus angle of attach

Fig. 26 (a) Open fan concept (b) Close fan concept

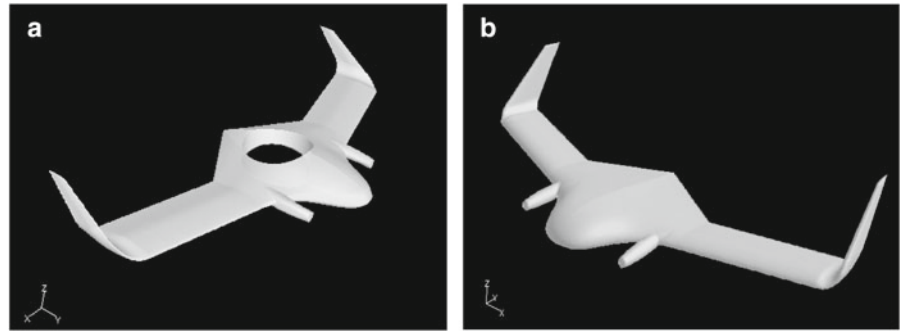


Fig. 27 Velocity vectors at fan gap $\alpha = 0^\circ$

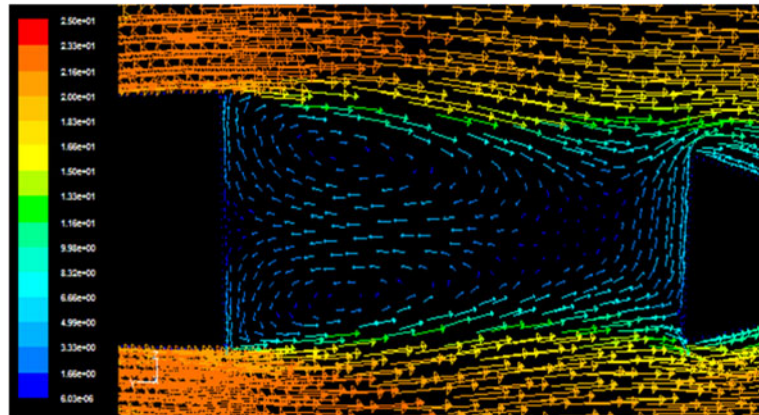


Fig. 28 Streamlines of close fan concept of TURAC at $\alpha = 5^\circ$

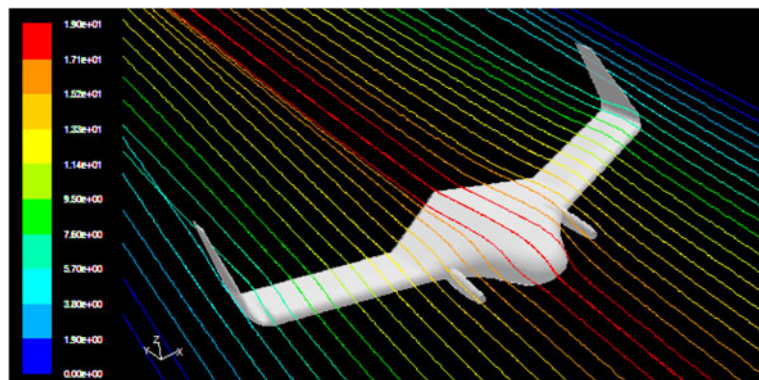
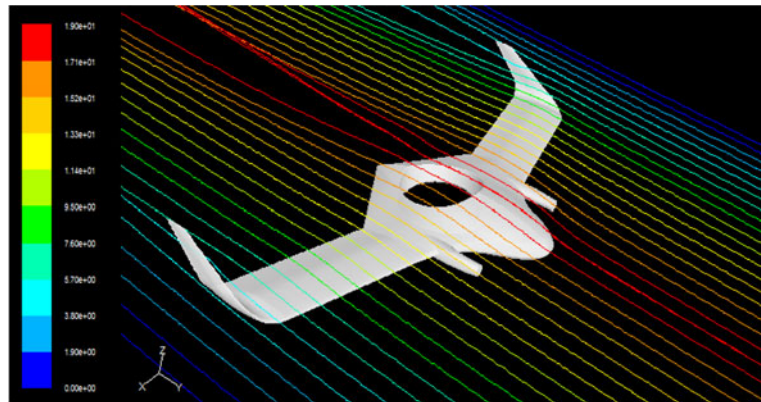


Fig. 29 Streamlines of open fan concept of TURAC at $\alpha = 5^\circ$



ter chord of the panel and reaches through trailing edge and infinite with the direction of freestream velocity. Control point on each panel is defined at three quarters chord of each panel. At each control point, Eq. 9 is applied as a boundary condition. The boundary condition is that freestream velocity component at the perpendicular of the surface is zero.

$$\nabla(\Phi_\infty + \Phi) \cdot \vec{n} = 0 \tag{9}$$

The values of horseshoe vortex are calculated by using Eqs. 10 and 11.

$$\left[\vec{v}_{11}\Gamma_1 + \vec{v}_{12}\Gamma_2 + \dots + \vec{v}_{1N}\Gamma_N + \vec{V}_\infty \right] \cdot \vec{n}_i = 0, \tag{10}$$

$i = 1, 2, 3, \dots, N$

$$\sum_{j=1}^N A_{ij}\Gamma_j = R_i \tag{11}$$

The developed code calculates C_L , C_{Dind} and C_M for various angles of attack. The change of C_L due to angle of attack can be seen in Fig. 24. The change of C_{Dind} due to angle of attack can be seen in Fig. 25. NACA 0015 symmetrical airfoil and NACA 34112 reflex airfoil, which is used at TURAC's geometry, are used for VLM calculations. C_L and C_{Dind} increase linearly due to angle of attack. The linear increase of C_L and C_{Dind} results from ignoring viscous effect at VLM.

3.2 CFD Analyses of TURAC

CFD analyses are achieved with open and close fan concept of TURAC (Fig. 26). In CFD model,

symmetry feature of TURAC is used, so half of geometry is meshed and analyzed to decrease the number of cells. At CFD analyses, realizable $k-\epsilon$ turbulence model with enhanced wall treatment is used. The definition at control volume is velocity inlet and pressure outlet; moreover, flow velocity is 20 m/s. At open fan concept, flow does not follow the surface through TURAC and vortices occur in the fan gap. The vortices can be seen clearly in Fig. 27. As an example, Figs. 28 and 29 shows the flow characteristics at an angle of attack of 0° and 5° for open and close fan concept of TURAC.

According to Table 12, open fan gap decreases C_L and increases C_D of TURAC. C_L and C_D increase with the increase of angle of attack at both open and close fan concept of TURAC. The analysis has led to design of fan doors to close in forward flight regime to increase lift coefficient and to decrease draft. The current work is focused on analyzing the propeller effect and the aerodynamic modeling of the transition flight.

Table 12 CFD results at 0° and 5° angles of attack

α ($^\circ$)		Open fan concept of TURAC	Close fan concept of TURAC
0°	C_L	0.0125	0.142
	C_D	0.0467	0.0266
	C_M	-0.0046	-0.0259
5°	C_L	0.3352	0.539
	C_D	0.065	0.0429
	C_M	0.0576	-0.079

Table 13 Wing modal analysis results

	Others (Hz) [22]	TURAC natural frequency (Hz)	Change in natural frequencies (Hz)
1st out-of-plane bending	13	11.82	9.07 %
1st torsional mode	46.3	45.58	1.55 %
2nd out-of-plane bending	87.69	81.63	6.91 %

4 Structural Design Features and Analysis of TURAC

For TURAC, composite material is favored to a large extent as flight vehicle material owing to its high strength and low weight. Outer shells of the wings and the body of the air vehicle are carved out using honeycomb structure between double-sided fibers. Aircraft support beams consist of tubes obtained from carbon fiber. Main beam and support beam, both of which stem from the wings, subside into beds inside the main body. This structure facilitates assembly and disassembly of the wings. Main bulk of the weight is gathered inside the body. These loads flow to outer shell of the body via frames inside the body.

For designing an aircraft that is sufficient in terms of structure that can endure maximum loadings to the aircraft, detailed finite element network of TURAC is created. Beams, ribs, and outer shells are the modeled main parts. In addition to these, motor, battery and electronic parts, which change vibration frequency considerably but do not have structural contribution, are modeled as concentrated mass [21], and their effect on aircraft's dynamic behavior is examined.

By modeling current configuration by finite element methods, it is controlled if the current configuration has sufficient strength for loadings. Structural analysis model of TURAC Unmanned Air Vehicle (UAV) is created, and material layout that can endure the maximum load to the structure is chosen. Aircraft design allows 3.8 g acceleration under elliptical loading.

Principally, a structurally adequate wing with enough stiffness is aimed. Wing is produced by calculating its natural frequencies and compared to other wings with similar size. In Table 13, results for TURAC and its comparison with other wings with similar size is shown. Results for the top three most important frequencies are shown. It is seen that there is less than 10 % in the wings in terms of natural frequency values.

In order to ensure structural sufficiency that is part of aircraft design cycle; position, geometry and material of support elements are chosen in such a way that it can endure maximum loads aircraft encounters.

Structural analyses are repeated to ensure the reliability of every section of the aircraft. As it can be seen in Fig. 30, as a result of the analyses, maximum deformation at the most critical flight regime is found to be 315 mm.

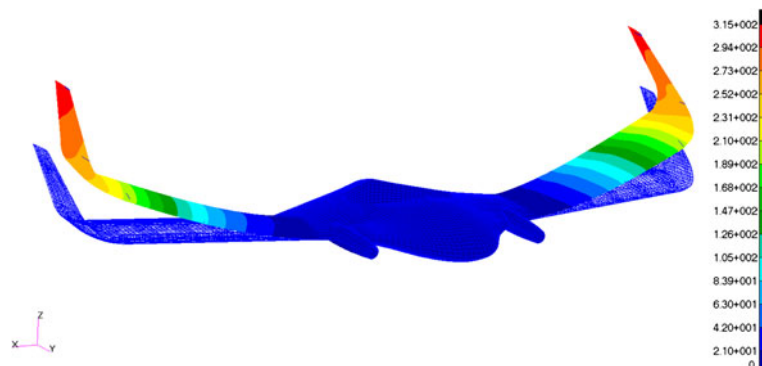
Fig. 30 Maximum displacement

Table 14 Material strength

Mechanical property	Mean value
Tensile strength (S_1)	431.5 MPa
Compression strength (S_{c1})	165.5 MPa
Shear stress (S_{12})	31.20 MPa

Maximum principal stress is 127 MPa at wing root lower shell, and minimum principal stress is 137 MPa at wing root upper shell. Both of the stress values are under the strength values, which are shown in Table 14.

At the lower part of wing root, maximum tensile strength is observed. Maximum principal stress distribution on the aircraft is shown at Fig. 31. The current design of TURAC can easily overcome the calculated maximum stresses.

Following the success of ITU Tailless UAV [23], prototype of TURAC has been produced (Fig. 32). First flight tests are performed by using this prototype of TURAC (Fig. 33) for not only to verify the concept but also to verify the structural calculations.



Fig. 32 Prototype of TURAC

5 Avionics System Design

5.1 General System Design

The general avionics system and the ground station is illustrated in Fig. 34. Ground station consists of radio command controlled by the operator, a ruggedized laptop used for loading mission

Fig. 31 Maximum and minimum principle stresses

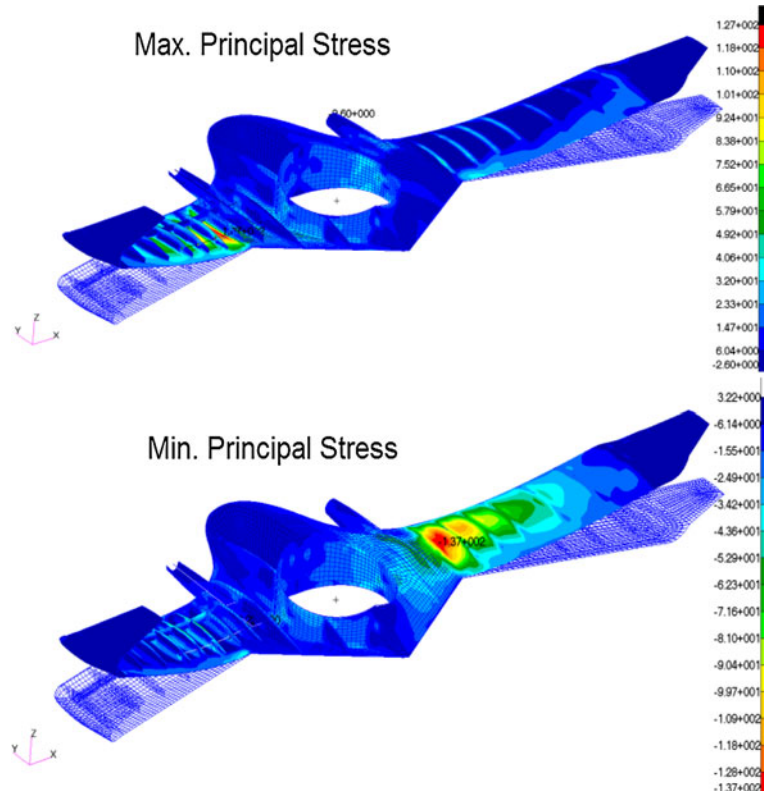




Fig. 33 Flight tests of TURAC prototype in ITU stadium

and monitoring vehicle status, and dual transceivers connected to this laptop. For operating the autonomous vehicle, there is a payload software, mission management software, and flight and health monitoring software running on the computer. Also the operator can control the vehicle manually by using remote control transmitter at the ground station.

On the air vehicle, there are flight control computer, which controls all of the segments of the autonomous flight, sensors with temperature compensators and filters, actuators, radio transceivers, mission management computer and payload system. All of the peripheral units communicate with flight control computer.

5.2 General Command and Control Scheme

Control system consists of mission management computer and flight control computer as seen in Fig. 35. Flight computer carries out missions with its position and orientation controllers. In addition the controller rather this be a computer or an actual operator can be changed with a switching mechanism.

Mission management computer aims to plan missions through navigation patterns and waypoints, which are either loaded previously or chosen at any given time through the ground station operator. While the vehicle is at full autonomous mode, position, speed, altitude and heading

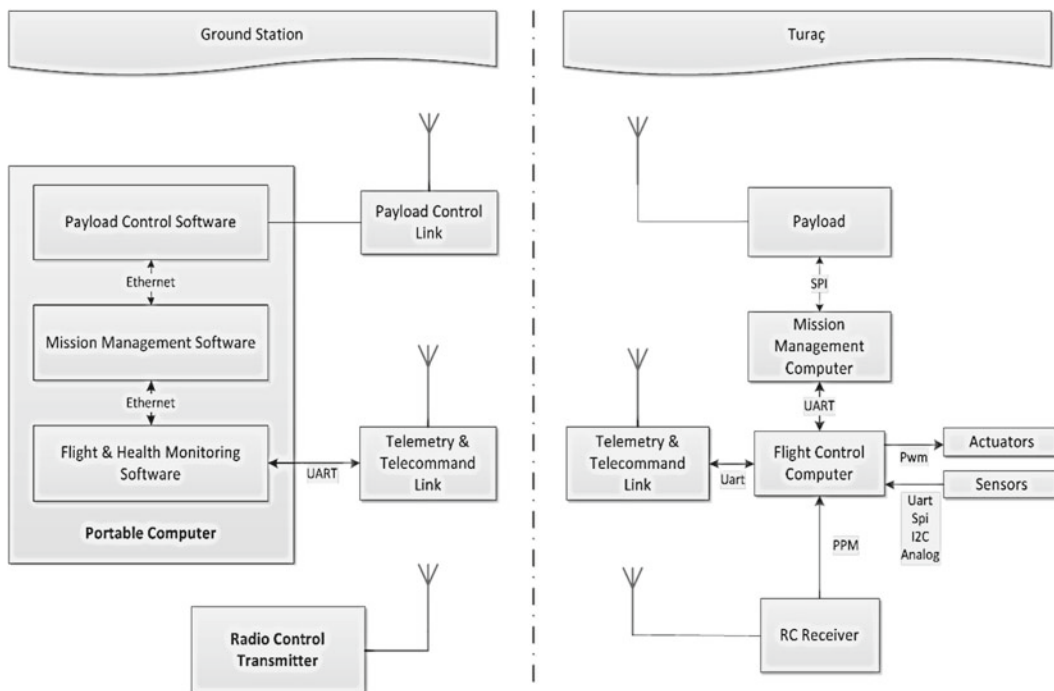
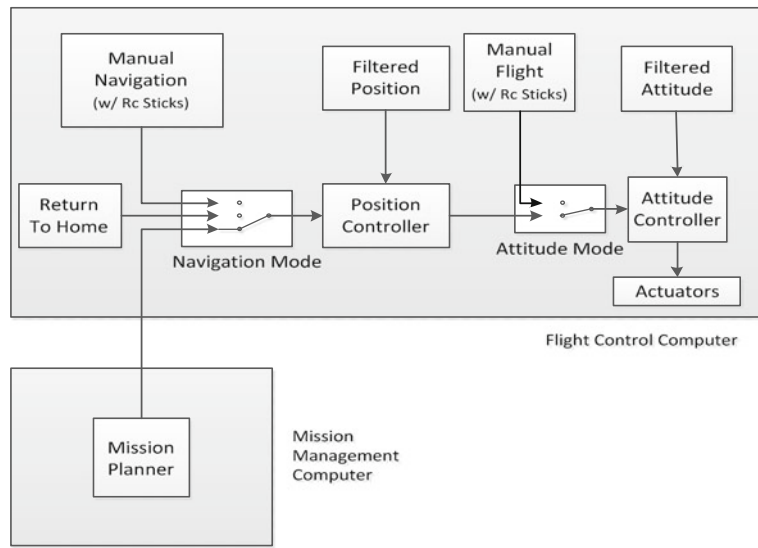


Fig. 34 General avionics system diagram

Fig. 35 General command and control diagram



angle are commanded by the mission management computer.

5.3 Flight Control Computer

Flight control computer carries out all types of low level tasks such as orientation and position

control of the flight vehicle, communication, data recording, battery control, and actuator control.

As it can be seen from Fig. 36, communication systems and INS communicate over UART, remote control receiver communicate over PPM, actuators communicate over PWM, MicroSD communicate over SDIO, a variety of other sensors communicate over analog, and high level mission

Fig. 36 Flight control computer

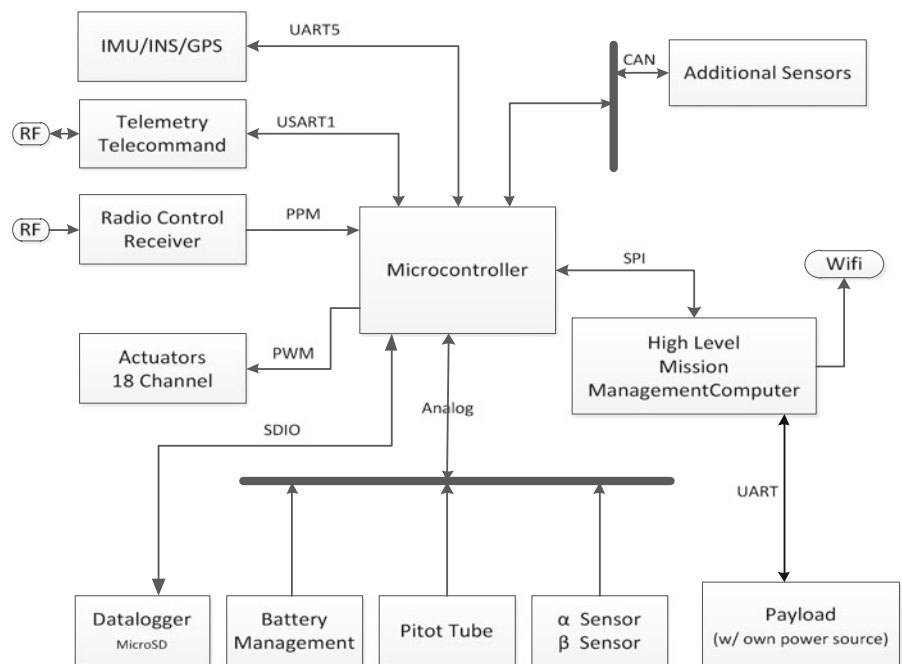
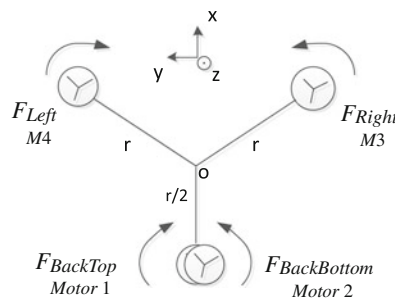
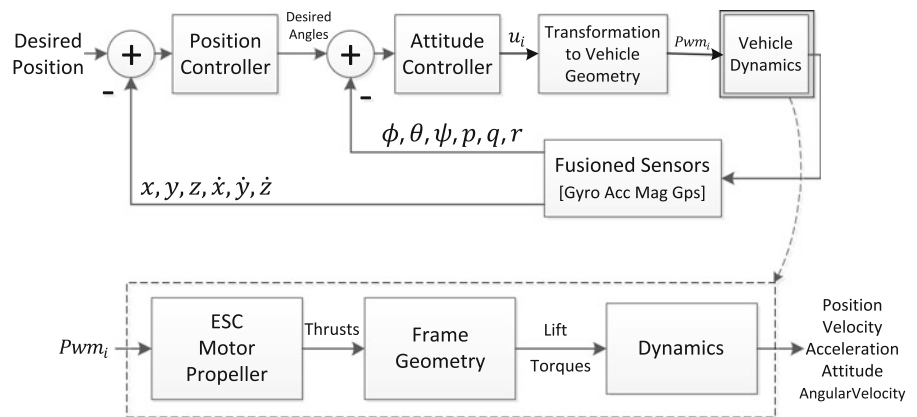


Fig. 37 General control system diagram and frame geometry



control computer communicate over SPI. In addition to these, there is a CANBus structure for possible sensors in future.

5.4 Flight Controller

Control scheme on flight control computer can be seen at Fig. 37.

Control structure consists of cascade controllers. Position information, which is specified by the operator manually or by mission management computer, is processed by position controller and converted to orientation information required by flight vehicle. Position information required by flight vehicle is converted to control signal with the help of a controller. These control signals are then converted to PWM signals that will control actuators according to the flight vehicle's geometry. This loop continues and flight vehicle reaches to desired positions. Orientation and position information of the vehicle is estimated precisely with the help of INS, which arise

from the fusion of IMU and GPS, and it provides feedback to the controllers. Manual flight tests including the stability augmentation system for hovering flights have been successfully performed on a basic tri-copter skeleton prototype of TURAC which includes the front rotors and the main coaxial lifting fan.

6 Conclusion

In this study, a commercial and multi-functional VTOL UAV with detachable and interchangeable wings is designed. The designed vehicle can carry payloads up to 8 kg for over 3 h while operating within a 35 km operational radius. In addition, the fixed wing TURAC vehicle has capability to transition between high speed forward flight and hover regime depending on the mission profile.

An iterative design process including trade-off studies, aerodynamic and structural analysis was

performed to reach the optimal size of the TURAC with a MTOW 45 kg and a wing span of 4.2 m. Functional prototypes were built to show success of the design at both hover and forward flight regime. Current work focuses on the building of the full flight test prototype of the TURAC UAV and aerodynamic modeling and control design for fully autonomous transition flight.

References

- Sarris, Z.: Survey of UAV Applications in Civil Markets. Technical University of Crete (2001)
- Quick, D.: Israel Aerospace Industries Unveils Tilt-rotor Panther UAV Platform. AERO GIZMO (2010)
- Dhaliwal, S.S.: Control of an Unconventional Double-Ducted Fan VTOL UAV for Obstructed Environments using the MARC System. MSc. Thesis., University of Calgary (2009)
- Zongjian, L.: UAV for mapping – low altitude photogrammetric survey, the international archives of the photogrammetry. In: Remote Sensing and Spatial Information Sciences, vol. XXXVII. Part B1, Beijing (2008)
- Watts, A.C., et al.: Small unmanned aircraft systems for low – altitude aerial surveys. *J. Wildl. Manag.* **74**(7), 1614–1619 (2010)
- Puri, A.: Survey of Unmanned Aerial Vehicles (UAV) for Traffic Surveillance. University of South Florida (2005)
- Charlie, J.K., Kevin, S.R., Rick, L.L., Steven, C.J., John, L.C.: Monitoring effects of a controlled subsurface carbon dioxide release on vegetation using a hyperspectral imager. *Intern. J. Greenhouse Gas Control* **3**(5), 626–632 (2009)
- Glenn, N.F., Mitchell, J.J., Anderson, M.O., Hruska, R.C.: Unmanned Aerial Vehicle (UAV) hyperspectral remote sensing for dryland vegetation monitoring. In: *Hyperspectral Image and Signal Processing: Evolution in Remote Sensing*, Shanghai, China (2012)
- Jay, S., Lawrence, R., Repasky, K., Keith, C.: Invasive Species Mapping Using Low Cost Hyperspectral Imagery. ASPRS (2009)
- Nansen, C., Sidumo, A.J., Capareda, S.: Variogram analysis of hyperspectral data to characterize the impact of biotic and abiotic stress of maize plants and to estimate biofuel potential. *Applied Spectrosc.* **64**(6), 627–636 (2010)
- Tindall, J.A.: Deconvolution of Plant Type (s) for Homeland Security Enforcement Using Remote Sensing on a UAV Collection Platform. Geological Survey Denver Co. (2006)
- Darvishsefat, A.A., Tobias, W.K., Klaus, I.I.: Application of hyperspectral data for forest stand mapping. In: *Symposium on Geospatial Theory, Processing and Applications*, Ottawa (2002)
- Tuominen, J., Lipping, T., Oy, P.: Detection of environmental change using hyperspectral remote sensing at Olkiluoto repository site. Working Report, Posiva Oy, Eurajoki, Finland (2011)
- Salem, F., Kafatos, M.: Hyperspectral image analysis for oil spill mitigation. In: *22nd Asian Conference on Remote Sensing*, Singapore, 5–9 November 2001
- Foy, B.W.: Hover Controls for a Unique Small-Scale Thrust Reversing UAV. MSc. Thesis, University of Colorado (2005)
- Frost and Sullivan: Study Analysing the Current Activities in the Field of UAV. European Commission, ENTR/2007/065 (2007)
- Ahn, O., Kim, J.M., Lim, C.H.: Smart UAV Research Program Status Update: Achievement of Tilt-Rotor Technology Development and Vision Ahead. In: *ICAS 2010, 27th International Congress of the Aeronautical Sciences* (2010)
- Smith, K.R., Belina, F.W.: Small V/STOL Aircraft Analysis, vol. 1. NASA Report CR-2425 (1974)
- Zhao, H.W.: Development of a Dynamic Model of a Ducted Fan VTOL UAV. MSc. Thesis, RMIT University (2009)
- Johnson, W.: NDARC - NASA design and analysis of rotorcraft theoretical basis and architecture. In: *NASA Ames Research Center, American Helicopter Society Aeromechanics Specialists' Conference*, San Francisco, CA, January (2010)
- MSC/NASTRAN Linear Static Analysis User's Guide for Version 69+. The MacNeal-Schwendler Corporation, Los Angeles, California (1997)
- Şahin, M., Sakarya, E., Ünlüsoy, L., İnsuyu, E.T., Seber, G., Özgen, S., Yaman, Y.: Design, analysis and experimental modal testing of a mission adaptive wing of an unmanned aerial vehicle. In: *UVW2010, International Unmanned Vehicle Workshop*, Paper ID: 10, 10–12 Haziran, HHO, İstanbul (2010)
- Karakaş, H., Koyuncu, E., ve İnalhan, G.: ITU Tailless UAV design. *J. Intel. Robotic Syst.* **69**, 131–146 (2013)